



Deposited via The University of Sheffield.

White Rose Research Online URL for this paper:

<https://eprints.whiterose.ac.uk/id/eprint/109099/>

Version: Accepted Version

Article:

Portius, P., Peerless, B., Davis, M. et al. (2016) Homoleptic Poly(nitrato) Complexes of Group 14 Stable at Ambient Conditions. *Inorganic Chemistry*, 55 (17). pp. 8976-8984.
ISSN: 0020-1669

<https://doi.org/10.1021/acs.inorgchem.6b01455>

This document is the Accepted Manuscript version of a Published Work that appeared in final form in *Inorganic Chemistry* © American Chemical Society after peer review and technical editing by the publisher. To access the final edited and published work see <https://doi.org/10.1021/acs.inorgchem.6b01455>.

Reuse

Items deposited in White Rose Research Online are protected by copyright, with all rights reserved unless indicated otherwise. They may be downloaded and/or printed for private study, or other acts as permitted by national copyright laws. The publisher or other rights holders may allow further reproduction and re-use of the full text version. This is indicated by the licence information on the White Rose Research Online record for the item.

Takedown

If you consider content in White Rose Research Online to be in breach of UK law, please notify us by emailing eprints@whiterose.ac.uk including the URL of the record and the reason for the withdrawal request.

Homoleptic poly(nitrato) complexes of Group 14 stable at ambient conditions

Peter Portius*, Benjamin Peerless, Martin Davis, Rory Campbell

Department of Chemistry, University of Sheffield, Brook Hill, Sheffield, S3 7HF, United Kingdom

Email: p.portius@sheffield.ac.uk

Abstract. Using a novel approach in homoleptic nitrate chemistry, the previously unknown hexanitrate complexes $\text{Si}(\text{NO}_3)_6^{2-}$ (**1c**), $\text{Ge}(\text{NO}_3)_6^{2-}$ (**2c**) as well as $\text{Sn}(\text{NO}_3)_6^{2-}$ (**3c**) were synthesised from the element tetranitrates as salt-like compounds which were isolated and characterised using ^1H , ^{13}C , ^{14}N and ^{29}Si NMR and IR spectroscopies, elemental and thermal analyses and single crystal XRD. All hexanitrates are moderately air sensitive at 298 K and possess greater thermal stability toward NO_2 elimination than their charge-neutral tetranitrato congeners as solids and in solution. The complexes adopt distorted octahedral coordination frameworks with geometries that are highly symmetric (**3c**) or deformed (**1c**, **2c**) depending on the degree of steric congestion of the ligand sphere. As opposed to the $\kappa^2\text{O},\text{O}'$ coordination mode reported for $\text{Sn}(\text{NO}_3)_4$ previously,¹ all nitrato ligands of **3c** coordinate in $\kappa^1\text{O}$ mode. Two experimentally observed and four additional geometric isomers of $\text{Si}(\text{NO}_3)_6^{2-}$ were identified as minima on the PES using DFT calculations at the B3LYP/6-311+G(d,p) level.

Introduction

Nitrogen and oxygen-rich nitric acid esters and other covalently bound nitrates are highly endothermic compounds. The covalent character of E–ONO₂ bonds causes a significant lowering of the activation barrier for the elimination of NO₂ in comparison to the NO₃[−] ion in salts. Intriguingly, polynitrato *complexes* occupy a place between these extremes. Such complexes and in particular the metal-containing species with bidentate nitrate ligand coordination, are powerful oxidising agents which is exemplified by the capability of Ti(NO₃)₄ to set alkanes on fire.² It has been shown previously that the thermal decomposition pathway of transition metal nitrato complexes leads to metals or metal oxides and involves multiple reaction steps in which highly reactive nitryl radicals, NO₃[·], or NO₂ are released depending on the coordination mode of the nitrato ligands.² It has been demonstrated that the anionic homoleptic nitrato complexes in the compounds (NO)Au(NO₃)₄, (NO)₂Pd(NO₃)₆ and (NO)₂Pt(NO₃)₆³ in which the nitrato ligands prevail in a monodentate mode produce metal in chemical vapour deposition (CVD) processes, whereas the compound (NO₂)Ga(NO₃)₄,⁴ in which a larger coordination centre permits agostic coordination of the nitrato ligand, generates gallium oxide deposits. Consequently, metal nitrates are considered in CVD applications for the growth of C,H-free deposits.⁴ The properties of complexes of

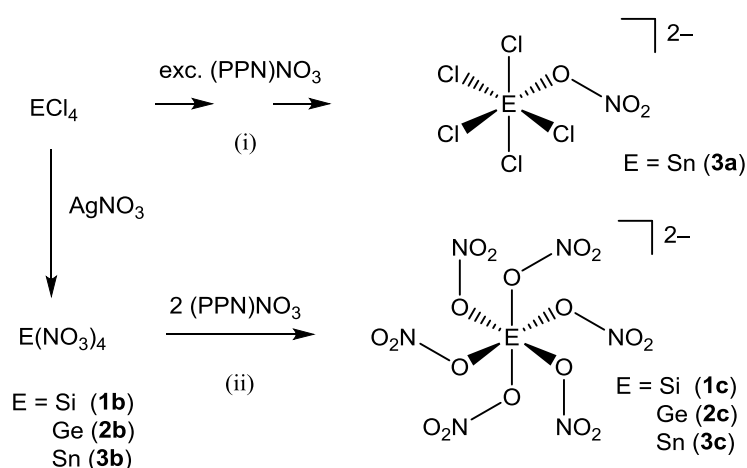
semimetallic *p*-block and *d*-block elements are related where the former possess, however, lower oxidation potentials and less labile NO₃ ligands. Polynitrato complexes of light *p*-block elements are interesting species that may act as unusual energetic materials and as novel precursors for well-defined E, N, O deposits. Such complexes are, however, not well-researched and many potentially viable complexes of elements with lesser metallic character are still unknown.

Traditionally, polynitrato complexes have been synthesised by the reaction of either N₂O₄ or N₂O₅ with metal halides.⁵ This method affords group 13, 14 and 15 polynitrato complexes of the type E(NO₃)₄ (E = Sn, **3b**⁶), E(NO₃)₄⁻ (E = B,^{7, 8} Al,⁹⁻¹³ Ga^{14,15}), E(NO₃)₅²⁻ (E = Al^{10,16-20}) and E(NO₃)₆^{q-} (E = Sn, *q* = 2;²¹ Al,^{22,23} Bi,²⁴ *q* = 3). Attempts to synthesise Pb(NO₃)₆²⁻, Ge(NO₃)₆²⁻ or Ge(NO₃)₄ (**2b**) using this method, however, failed and afforded GeO₂ and Pb(NO₃)₂, respectively, instead.²⁵ An alternative preparative method for polynitrates involving silver nitrate as a NO₃ group transfer reagent afforded **1b** from SiCl₄ in MeCN-Et₂O solution.²⁶ While data on homoleptic group 13 nitrato complexes and in particular those of B, Al and Ga and that of Sn(IV) (*vide supra*) is available, very little is known on complexes of the lighter group 14 elements Si and Ge. Data available thus far for group 14 nitrates suggest that poly(nitrato) silicon and germanium complexes are likely to be insufficiently stable to allow their isolation at r.t. – a notion which could be rationalised by estimating the degree of ionicity of the Si–O and Ge–O bonds in hypothetical E(NO₃)_x^{(4-x)-} complexes which should be less than that of the E–O bonds of the related and well-characterised complexes Al(NO₃)₄⁻, Ga(NO₃)₄⁻ and Sn(NO₃)₄ (**3b**). In these compounds the trigonal geometry of the NO₃ group is severely distorted through the shortening of the terminal N–O bonds and the lengthening of the N–O bond that links to the centre (E) *via* E–ONO₂ bridges. In group 14, **3b**^{1,27,28} and the salt-like compounds (Cat)₂Sn(NO₃)₆, Cat = Et₄N⁺,²¹ Cs⁺²⁵ remain the only characterised *homoleptic* nitrates. To the best of our knowledge, reported structures featuring any Si–ONO₂ or Ge–ONO₂ motifs are the nitric acid silyl-ester O₂NO–SiMe₂{C(SiMePh₂)(SiMe₃)₂}²⁹ and the five-coordinate nitrato complex Si(NO₃-κ¹O){O–C(Me)=CH–C(Me)=N–C₆H₄–S-κ³N,O,S}Ph,³⁰ while SiMe₂(NO₃)₂ and the Lewis acid base adduct Si(NO₃)₄·2py are the only characterised poly(nitrato) silicon compounds.²⁶ Si(NO₃)₄ (**1b**, *vide infra*) is proposed as an intermediate for the preparation of Si(NO₃)₄·2py; however, no spectroscopic evidence of its formation is available. Si(NO₃)₄·2py is highly thermolabile and releases nitrogen oxides readily at r.t. Although the germanium nitrates GeMe₃(NO₃) and GeMe₂(NO₃)₂^{27, 28, 31} have been reported, no reference has been made to either Ge(NO₃)₄ (**2b**) or Ge(NO₃)₆²⁻. Due to these findings,

covalent nitrates have been considered *a priori* unstable and their synthesis a considerable challenge.

This paper reports the first synthesis and the full characterisation of homoleptic silicon and germanium nitrates including the experimentally determined molecular structures $E(\text{NO}_3)_6^{2-}$, $E = \text{Si}, \text{Ge}$ or Sn . Detailed structural and reactivity studies reveal how the binding mode of the nitrate ligand affects stability and chemical properties of this class of compounds. Density functional theory methods were employed to evaluate the energetics of conformational isomers of $\text{Si}(\text{NO}_3)_6^{2-}$ complexes.

Results and Discussion



Scheme 1. Synthesis of the homoleptic nitrate complexes of silicon, germanium and tin. $(\text{PPh}_3)_2\text{N}^+$ (PPN^+) are counter ions to charged complexes.

In the exploration of potential routes for the synthesis of the hexanitrate complexes of silicon, germanium and tin, two approaches were taken. In a direct approach (*i*), a suitable halide is allowed to react with a large excess of nitrate salt of a non-coordinating cation avoiding the intermediate formation of the highly reactive charge-neutral tetranitrates. This method is akin to the synthesis of the related hexaazido complexes.³²⁻⁴⁶ The indirect approach (*ii*) involves the *in situ* formation of tetranitrates, which are then “trapped” by Lewis acid-base reactions with nitrate anions.

The feasibility of the $\text{Cl}^- / \text{NO}_3^-$ ligand exchange in approach (*i*) was tested by the reaction of tin(IV) chloride with an excess of NO_3^- ions (Scheme 1). The nitrate complexes of this element were deemed to be the thermally least labile target species. The addition of $(\text{PPN})\text{NO}_3$ to a solution of SnCl_4 in Ar-saturated acetonitrile at 60°C causes a brown

colouration of the protective gas which indicates the formation of NO_2 . The formation of NO_2 was confirmed by the presence of a band at 1740 cm^{-1} characteristic for NO stretches in the *in situ* IR spectra of the reaction solution. Moderately air sensitive, colourless, block-shaped crystals grow in the concentrated reaction solution below -20°C and these were investigated by single crystal X-ray diffraction. The structure solution revealed that the mixed-ligand complex in the salt $(\text{PPN})_2[\text{SnCl}_5(\text{NO}_3)]$ (**3a**) had formed as one of the reaction products. The molecular structure of the $\text{SnCl}_5(\text{NO}_3)^{2-}$ complex in **3a** is shown in Fig. 1; complete structural details are given in the SI. Briefly, $\text{SnCl}_5(\text{NO}_3)^{2-}$ adopts a distorted octahedral geometry with a long Sn–Cl bond (2.58 \AA) *trans* to the nitrate ligand and two short Sn–Cl bonds (2.41 \AA) due to the variation in the *trans* influence of chloro and nitrate ligands. The nitrate ligand binds through one oxygen atom ($d_{\text{Sn-O}} = 2.16\text{ \AA}$) which is located off the Sn–Cl_{*trans*} axis. A Sn–O–N angle of 133° implies that a second oxygen atom is drawn close to the coordination centre $d(\text{Sn}\cdots\text{O}) \approx 3.1\text{ \AA}$. Due to the type of disorder in the tin-containing part of the crystal it is clear that the observed diffraction pattern cannot be caused by a disordered solid solution containing an equal distribution of SnCl_6^{2-} and $\text{Sn}(\text{NO}_3)_2\text{Cl}_4^{2-}$. Heating an acetonitrile solution containing **3a** and a tenfold molar excess of $(\text{PPN})\text{NO}_3$ to $60\text{ }^\circ\text{C}$ led to a brown solution from which no products other than $(\text{PPN})_2[\text{SnCl}_5(\text{NO}_3)]$ and $(\text{PPN})\text{NO}_3$ were obtained. The absence of a nitrate-rich stannate indicates that these complexes tend to decompose upon release of NO_2 under the conditions needed to bring about ligand exchange using nitrate salts with weakly coordinating cations. Therefore, the Cl / NO_3 ligand exchange cannot be driven to completion in a hexacoordinate tin complex under this regime.

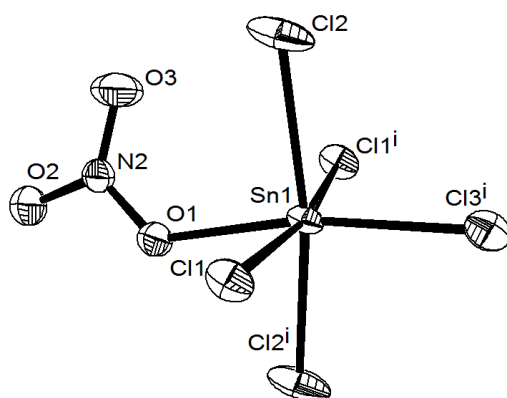


Figure 1. Thermal ellipsoid plot of one component of the disordered structure of $[\text{SnCl}_5(\text{NO}_3)]^{2-}$ in compound **3a** at 100 K. Ellipsoids are set to 50% probability. Selected bond lengths [\AA] and angles [$^\circ$]: Sn1–Cl1 2.423(15), Sn1–Cl2 2.357(15), Sn1–Cl3 2.395(3), Sn1–O1 2.155(4), O1–N2 1.287(9), O2–N2 1.240(13), O3–N 21.217(11); Sn1–O1–N2 128.8(7), Cl1–Sn1–Cl1 169.79(3), Cl1–Sn1–Cl2 91.89(5), Cl1–Sn1–O1 87.89(10), Cl2–Sn1–O1 79.27(16), Cl2–Sn–Cl2 170.20(3), Cl2–Sn1–Cl3 95.31(8), O3–N2–O2 121.2(7), O3–N2–O1 121.4(11), O2–N2–O1

117.3(9). Atomic coordinates denoted with superscript (i) were generated by inversion symmetry from the asymmetric unit.

Exploring route (ii), tin tetranitrate (**3b**) that was obtained from the reaction of SnCl₄ with AgNO₃,¹ was allowed to react with (PPN)NO₃ in an acetonitrile solution at 0°C. *In situ* IR spectroscopy revealed a reaction that causes the bands due to the characteristic N–O stretch of **3b** at 1556 cm⁻¹ to disappear while bands of a new NO₃ species appeared at lower wavenumbers (e.g. 1547 cm⁻¹). A colourless crystalline solid was obtained from the reaction mixture, which according to ¹H, ¹³C, ³¹P and ¹⁴N NMR and IR spectra, elemental analysis, and X-ray diffraction data is identifiable as the hexanitratostannate(2-) (PPN)₂Sn(NO₃)₆ (**3c**).

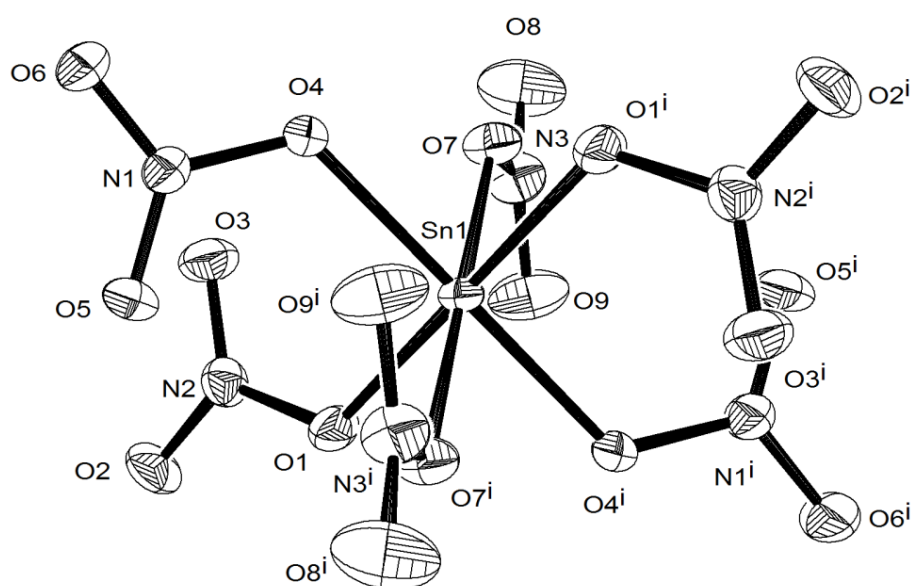


Figure 2. Thermal ellipsoid plot of the hexa(nitrato)stannate(2-) complex in (PPN)₂Sn(NO₃)₆·2MeCN (**3c**·2MeCN) at 100 K. Ellipsoids are set to 50% probability. Selected bond lengths [Å] and angles [°]: Sn1-O1 2.0624(17), Sn1-O7 2.0706(16), Sn1-O4 2.0831(16), O1-Sn1-O1ⁱ 180, O1-Sn1-O7 80.79(7), O1-Sn1-O7 99.21(7), O7-Sn1-O7ⁱ 180, O1-Sn1-O4 78.79(6), O1-Sn1-O4 101.21(6), O7-Sn1-O4 79.17(7), O7-Sn1-O4 100.83(7); Sn1 occupies an inversion centre. Atomic coordinates denoted with superscript (i) were generated by inversion symmetry from the asymmetric unit.

The anionic part of the crystal structure of **3c** (Fig. 2) consists of a *D*_{3d} symmetric tin(IV) complex in which six nitrate ligands coordinate *via* comparably long Sn–O bonds ($d(\text{Sn–O}) = 2.0624(17)\text{--}2.0831(16)$ Å) which are, intriguingly, on average shorter than those found in Sn(NO₃)₄ (**3b**, 2.151(7)–2.195(7) Å) even though the number of coordinated nitrate ligands is smaller in the latter. The octahedral SnO₆ coordination framework in **3c** is elongated along one *C*₃ axis. The distortion is caused by crowding of the ligand sphere due to the essentially covalent nature of the coordinative bonds which appear to involve *sp*² hybridisation of the ligating oxygen and therefore require a non-linear ligand coordination (Sn–O–N angles of 120° required, 121.9(1)–123.0(1)° observed). This coordination angle brings six additional

potential ligators into closer proximity of the centre and causes additional $\text{Sn}\cdots\text{NO}_3$ interactions ($d(\text{Sn}\cdots\text{O}) = 3.105$ to 3.121 Å) which elongate the SnO_6 octahedron along the axis normal to the face defined by O1, O4 and O7 and reduce the adjacent O–Sn–O bond angles from their ideal value of 90° down to $78.79(6)$ – $80.79(7)^\circ$ (see Fig. 2, caption and Table 1). Hence the $\kappa^1\text{O}-\text{NO}_3$ coordination mode of the nitrate ligands in **3c** is in stark contrast to the bidentate $\kappa^2\text{O},\text{O}'-\text{NO}_3$ mode found in **3b** which possesses an eight-coordinate Sn centre (see ref. 1 for the crystallographically determined structure of **3b**). Compound **3c** is moderately air sensitive and soluble in CH_2Cl_2 and MeCN. No decomposition was detected over 15 minutes in a MeCN solution at temperatures of up to 35 – 40°C . A comparison of solution IR spectra with those obtained from nujol suspension indicate that $\text{Sn}(\text{NO}_3)_6^{2-}$ does not dissociate into $\text{Sn}(\text{NO}_3)_4$ in solution.

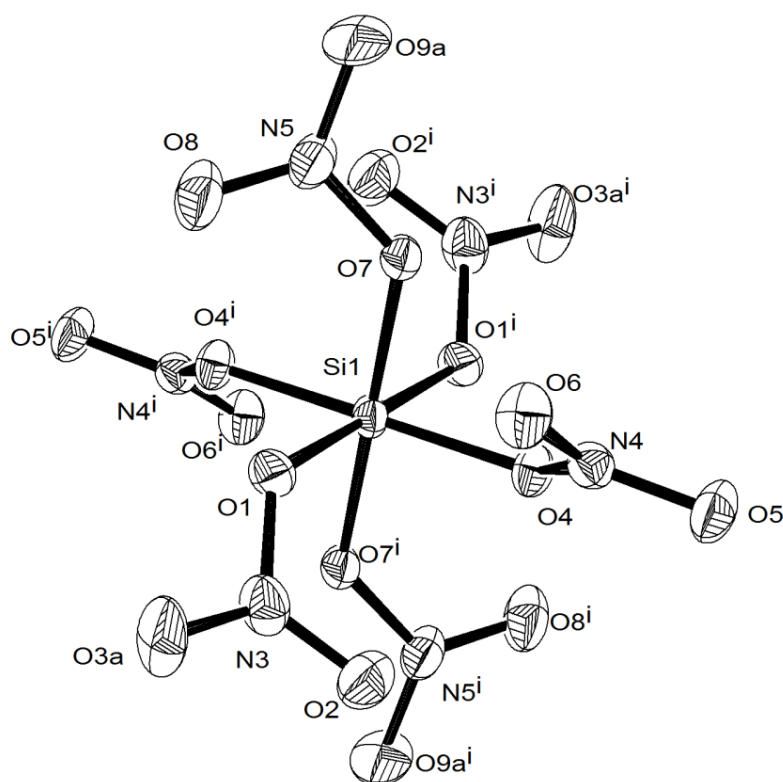


Figure 3. Thermal ellipsoid plot of one component of the two crystallographically independent hexa(nitrato)silicate(2[−]) complexes in crystals of **1c** at 100 K. Ellipsoids are set to 50% probability. Selected bond lengths [Å] and angles [°]: Si1–O1 1.7875(16), Si1–O4 1.7936(14), Si1–O7 1.7689(15), Si2–O16 1.7785(16), Si2–O10 1.773(15), Si2–O13 1.8053(15); O1–Si1–O1 180, O1–Si1–O4 96.13(7), O1–Si1–O4ⁱ 83.87(7), O4–Si1–O4 180, O1–Si1–O7 90.78(7), O1–Si1–O7ⁱ 89.22(7), O4–Si1–O7 88.19(7), O4–Si1–O7ⁱ 91.81(7), O7–Si1–O7ⁱ 180, O16–Si2–O16ⁱ 180, O16–Si2–O10 87.52(7), O16–Si2–O10ⁱ 92.48(7), O10–Si2–O10ⁱ 180, O16–Si2–O13 89.14(7), O16–Si2–O13ⁱ 90.86(7), O10–Si2–O13 82.27(7), O10–Si2–O13ⁱ 97.73(7), O13–Si2–O13ⁱ 180. Disorder in N–O groups is accounted for by a 1:1 disorder model for two independent NO_3 ligands in which the positions of the terminal O atoms are split and geometry and thermal motion related to each other by suitable SADI, SIMU and DELU restraints. Atomic coordinates denoted with superscript (i) were generated by inversion symmetry from the asymmetric unit.

Previous work led to the suggestion that the classical $\text{N}_2\text{O}_5 / \text{EX}_n$ method used for binary nitrates is unsuitable for the synthesis of the unknown germanium tetranitrate, $\text{Ge}(\text{NO}_3)_4$ (**2b**), as attempts to prepare **2b** led to GeO_2 .²³ We have instead applied the method used for the *in situ* generation of the lighter congener, $\text{Si}(\text{NO}_3)_4$ (**1b**), with the intention to obtain a Lewis acid precursor and facilitate a reaction of **2b** with nitrate anions under conditions similar to those for **3c**. It was found that GeCl_4 reacts with AgNO_3 in MeCN solution at r.t. causing the immediate precipitation of AgCl. An acetonitrile adduct, $\text{Ge}(\text{NO}_3)_4 \cdot \text{MeCN}$ (**2b.MeCN**), remains after evaporation of the filtered, colourless reaction solution. While the colourless, waxy **2b.MeCN** melts under decomposition at 30-35°C releasing a brown gas, the gas evolution in MeCN solutions at r.t. becomes noticeable in the protective atmosphere of the storage vessel after at least 6 h. **2b** has characteristic NO_2 absorption bands in the IR spectrum at 1618 and 1558 cm^{-1} and 1286 cm^{-1} . Based on interpretations of infrared spectra of nitrate complexes in the cited literature, these bands are assigned to the asymmetric and symmetric N–O bond stretching vibrations $\nu_{\text{as}}(\text{NO}_2)$ and $\nu_{\text{s}}(\text{NO}_2)$, respectively. MeCN solutions of **2b** react with $(\text{PPN})\text{NO}_3$ in an analogous fashion to **3b**, generating the salt $(\text{PPN})_2[\text{Ge}(\text{NO}_3)_6]$ (**2c**), which was isolated as colourless, less air sensitive crystals that are stable at ambient temperature. The preparation of the highly thermolabile $\text{Si}(\text{NO}_3)_4$ (**1b**) involved SiCl_4 that had to be dissolved in diethyl ether in order to bring about the reaction with AgNO_3 . Using acetonitrile as the solvent resulted in no precipitation of AgCl over the period of several hours. The same method described for **2c** and **3c** was then used to convert (**1b**) into $(\text{PPN})_2[\text{Si}(\text{NO}_3)_6]$ (**1c**), which shows no decomposition over several months at a temperature of -28 °C, though the crystals begin to discolour within few hours at ambient temperature. The application of method (i) to synthesise **1c** resulted in the type of decomposition observed for **3c**. The structures of the salts **1c** (Fig. 3) and **2c** (Fig. 4) were also determined by single crystal X-ray diffraction studies.

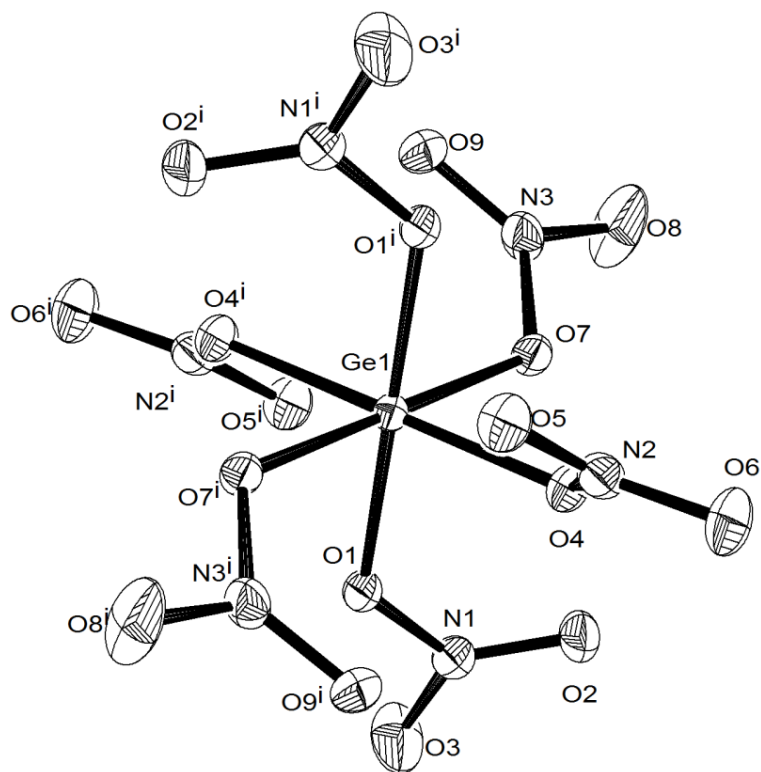


Figure 4. Thermal ellipsoid plot of one crystallographically independent hexanitrate germanate(2⁻) complex in crystals of **2c** at 100 K. Ellipsoids are set to 50% probability. Selected bond lengths [Å] and angles [°]: Ge1-O7 1.8918(12), Ge1-O1 1.8944(13), Ge1-O4 1.9166(12), Ge2-O10 1.8794(13), Ge2-O16 1.8988(13), Ge2-O13 1.9062(12); O7-Ge1-O7ⁱ 180, O7-Ge1-O1 86.43(5), O7-Ge1-O1ⁱ 93.57(5), O1-Ge1-O1ⁱ 180, O7-Ge1-O4 99.69(5), O7-Ge1-O4ⁱ 80.31(5), O1-Ge1-O4 91.60(5), O1-Ge1-O4ⁱ 88.40(5), O4-Ge1-O4ⁱ 180, O10-Ge2-O10ⁱ 180, O10-Ge2-O16 91.47(6), O10-Ge2-O16ⁱ 88.53(6), O16-Ge2-O16ⁱ 180, O10-Ge2-O13 92.59(6), O10-Ge2-O13ⁱ 87.41(6), O16-Ge2-O13 82.37(6), O16-Ge2-O13ⁱ 97.63(6), O13-Ge2-O13ⁱ 180. Atomic coordinates denoted with superscript (i) were generated by inversion symmetry from the asymmetric unit.

A comparison of the structural parameters derived from the X-ray diffraction studies reveals a number of interesting trends (Table 1). Even though all hexa(nitrate)complexes E(NO₃)₆²⁻ (E = Si, Ge, Sn) possess strict inversion symmetry and therefore all *trans*-ligand pairs are in the *anti*-conformation (*vide infra*), the relative orientation of the ligand pairs differ and this results in different complex geometries. While those in **1c** and **2c** can be approximated by C_{2h} point group symmetry, in **3c** an orientation close to D_{3d} is adopted. Consequently, the coordination centre in the former complexes is not in the planes spanned by all individual NO₃ ligands. A comparison of the inter-ligand O–E–O bond angles reveals deviations from 90° that increase in the series Si(NO₃)₆²⁻, Ge(NO₃)₆²⁻, Sn(NO₃)₆²⁻ causing extended distortions of the [EO₆] framework (*vide supra*). The average E–O–N angles, however, narrow in this series and get very close to the value required for sp² hybridised oxygen in **3c**. The change of angle is interpreted in terms of increased crowding of the ligand spheres. All E–O bonds are long in comparison with most four-coordinate complexes and this is ascribed to the typical bond-elongating effect upon hyper-coordination. More subtle changes are noticeable

in the intra-ligand bonds where the internal N–O bonds are much longer, and the external N–O bonds slightly shorter than those of the uncoordinated NO_3^- ion. All intramolecular Sn–O distances to the *endo* terminal oxygen atoms, $d(\text{E}\cdots\text{O})$, are 0.5 to 0.6 Å shorter than the sum of the van der Waals radii.⁴⁷

Table 1. Characteristic bond length ranges [Å] and angles [°] in the $\text{E}(\text{NO}_3)_n^{(4-n)2-}$ complexes of **1c-3c** ($n = 6$) and **1b** ($n = 4$)

	$d(\text{E}-\text{O})^a$	$d(\text{E}\cdots\text{O})^b$	$d(\text{O}-\text{N})_{\text{int}}$	$d(\text{O}-\text{N})_{\text{term}}$	$\angle(\text{E}-\text{O}-\text{N})$	$\angle(\text{O}-\text{E}-\text{O})^c$	
1c	1.769(2)- 1.805(2)	3.082- 3.174	1.342(2)- 1.352(2)	1.204(2)- 1.235(4)	127.2(2)- 130.6(2)	82.27(7)- 97.73(7)	XRD ^d
1c (S_6)	1.809	3.172	1.342	1.216, 1.224	131.5	87.2, 92.8	DFT ^e
1c (C_{2h})	1.802, 1.818	3.136, 3.204	1.338, 1.347	1.212- 1.225	129.4, 133.3	83.5- 96.5	DFT ^e
1c (C_{2h})	1.798, 1.814	3.125, 3.195	1.342, 1.346	1.213- 1.220	129.0, 133.1	83.6- 96.4	DFT ^{e,f}
1b (S_4)	1.667	2.901	1.462	1.185, 1.200	122.5	117.9	DFT ^{e,f}
2c	1.879(2)- 1.917(2)	3.094- 3.193	1.338(2)- 1.356(2)	1.201(2)- 1.223(3)	122.9(1)- 128.1(1)	82.4(1)- 99.7(1)	XRD ^d
3c	2.062(2)- 2.083(2)	3.105- 3.121	1.329(2)- 1.334(3)	1.207(3)- 1.225(2)	121.9(1)- 123.0(1)	78.8(1)- 101.2(1)	XRD ^d
NO_3^-	-	-	-	1.226(3)- 1.268(3)	-	-	XRD ^{d,e}

^a e.s.d.s < 0.002 are rounded up, ^b sum of van der Waals radii E, O / Å: 3.62 (E = Si); 3.63 (E = Ge), 3.69 (E = Sn);^{47,48} ^c all *trans* O–E–O angles equal 180°; ^d determined crystallographically, ^e density functional theory at the B3LYP/6-311+G(d,p) level, ^f PCM (MeCN); ^g obtained from (PPN) $\text{NO}_3 \cdot \text{MeCN}$, crystallographic data can be found in the SI.

Thermogravimetric analyses of compounds **1c-3c** (TGA, Fig. 5) suggest the operation of a three-stage thermolysis process. The onset of decomposition of **1c** occurs at $T_{\text{on1}} = 138^\circ\text{C}$ (stage I, 12.7 % mass loss) and is followed by the stages II ($T_{\text{on2}} = 257^\circ\text{C}$, 2.0 %) and III ($T_{\text{on3}} = 398^\circ\text{C}$). The mass loss up to 300 °C integrates to 14.8%. Similar observations were made with **2c** where T_{on1} was found to be only slightly higher (145°C, 12.0 %) whereas the onset for stage II occurred at the same temperature within the accuracy of measurement ($T_{\text{on2}} = 260^\circ\text{C}$, 4.2 %). The mass loss regime of compound **3c·2MeCN** is analogous to that of **1c** and **2c** with the exception of crepitation occurring at $T_{\text{on}} = 93^\circ\text{C}$ and the onset temperatures for stages I and II being higher (204°C and 303°C). The elevated onset temperature for thermal decomposition are remarkable given the thermal sensitivity of the polynitrato complexes formed during $\text{Cl}^- / \text{NO}_3^-$ ligand exchange reactions (*vide supra*). The thermal reactivity is reflected in differential scanning calorimetry traces which indicate the exothermic nature of stage I (Fig. 5). Furthermore, heating crystals of **1c** or **2c** to 160°C under a dynamic vacuum releases brown gas. A comparison of IR spectra of the yellow, glassy residues left behind

with those of a genuine sample indicate that (PPN)NO₃ is formed at this temperature. Only the residue of **1c** shows additional signatures of a species bearing nitrate ligands.

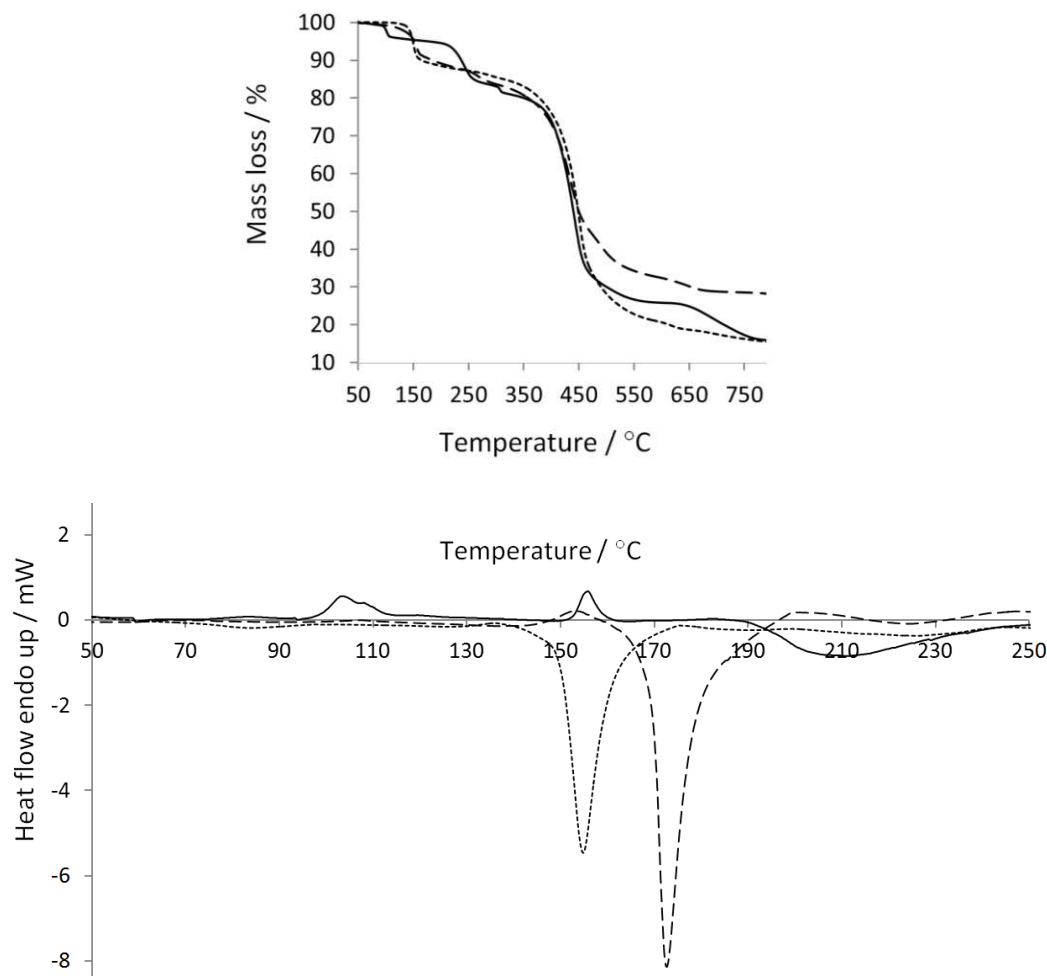


Figure 5. Thermogravimetric (top) and calorimetric traces (bottom) of the (PPN)₂E(NO₃)₆ salts **1c** (E = Si, - - -), **2c** (E = Ge, - · - ·) and **3c** **2MeCN** (E = Sn, —) obtained with heating rates of 10 K min⁻¹.

The available data can be interpreted tentatively in terms of NO₂ and O₂ gas release assuming that by completing stage II the decomposition reaction (PPN)₂E(NO₃)₆ → 2(PPN)NO₃ + EO_n + 4NO₂ + (1 - n/2)O₂ is complete. This scheme reproduces the observed mass losses very well (**1c**, *n* = 2, Δ*m* / (%) = 14.8 predicted, 14.6 observed; **2c**, *n* = 0, 16.3, 16.3; **3c**, *n* = 1, 14.8, 14.9) and implies the formation of SiO₂, Ge and SnO, respectively. Furthermore, all stage I mass losses are commensurate with the release of approximately four molar equivalents of NO₂ (**1c**, Δ*m* / (%) = 12.4 predicted, 12.7 observed; **2c**, 12.0, 12.1; **3c**, 12.0, 11.7).

Density functional theory calculations at the B3LYP/6-311+g(d,p) level on both Si(NO₃)₆²⁻ and Si(NO₃)₄ systems offer explanations for the increased thermal stability of the six-coordinate in comparison to four-coordinate nitrate complexes. A large difference was found

in the internal bonds N-O which are 0.1 Å longer in **1b** (see Table 1) and in charge distribution where less negative charge is distributed over the NO₃ ligands in **1b**. These changes have the effect of increasing the strength of the terminal N-O bonds and this is reflected in the vibrational frequencies $\nu_{\text{as}}(\text{NO}_2)$ which is more than 100 cm⁻¹ higher in **1b** (see experimental part and DFT results, table 2). These characteristics position the structure of **1b** closer to the transition state for NO₂ elimination than **1c**. An in-depth investigation revealed that six isomers of hexa(nitrato)silicate complex are likely to have stable geometries (Fig. 6). These isomers differ primarily in their relative *trans*-(O₂NO)-E-(ONO₂) ligand conformations which were found to be *syn, syn, syn* (C₃), *syn, syn, anti* (C₂), *syn, anti, anti* (C_s) and *anti, anti, anti* (C_{2h}, S₆ and D_{3d}) (point group symbols in parentheses).

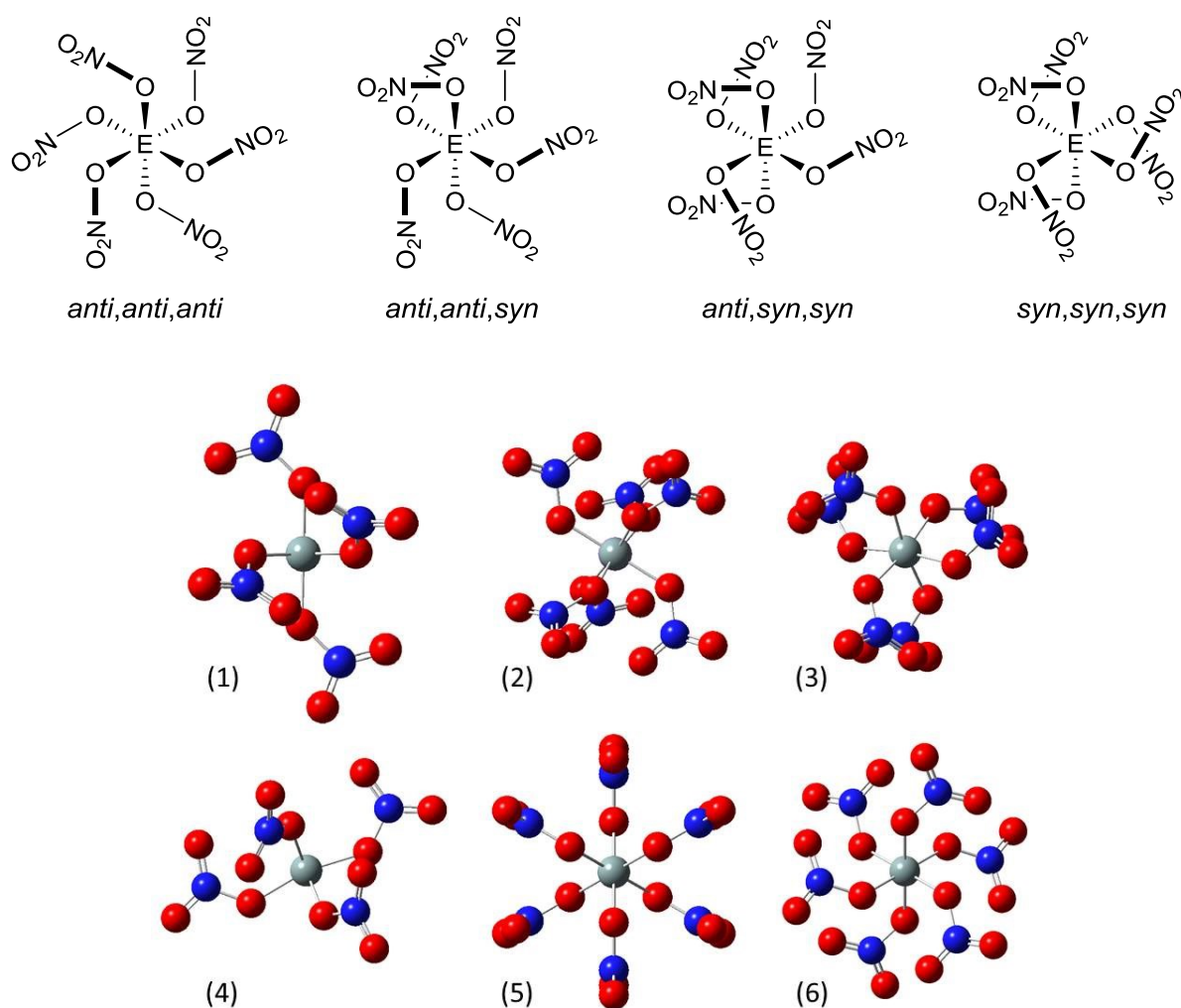


Figure 6. Stereo projections of the *syn* / *anti* conformers of Si(NO₃)₆²⁻ (top, labels denote relative orientation of the *trans*-pairs) and ball-and-stick diagrams (bottom) of the optimised geometries obtained from DFT calculations at the B3LYP/6-311+g(d,p) level with the PCM model (MeCN) and the following start geometries applied: C_{2h} (1), C₂ (2), C₃ (3), C_s (4), D_{3d} (5) and S₆ (6) (blue, N; red, O; grey, Si).

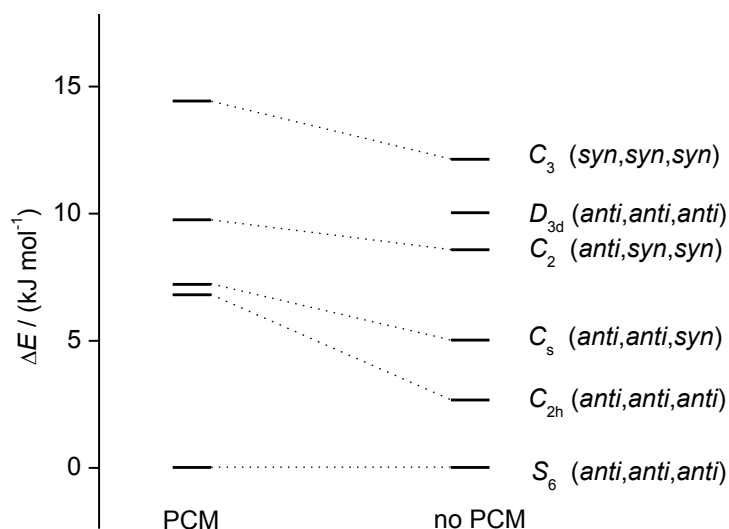


Figure 7. Total energies (0 K) relative to the lowest-energy isomer of the optimised geometries at the B3LYP/6-311+g(d,p) level. In the polarisable continuum model (PCM with MeCN as solvent, left), the D_{3d} symmetric conformer is not a minimum on the PES.

With the exception of the D_{3d} symmetry, for which one imaginary frequency was found, all conformer models lead also to stable minima upon taking account of solvent (MeCN) within the polarisable continuum model (PCM). From a comparison of the energies (Fig. 7 and Table 2), a clear trend emerges that inversely correlates total energy with the number of *anti*-configured *trans*-ligands.

Table 2. Total energies E_{tot} / (kJ mol⁻¹)^a of the $\text{Si}(\text{NO}_3)_6^{2-}$ species relative to the S_6 symmetric conformer and the frequencies of the fundamental $\nu_{\text{as}}(\text{NO}_2)$ N-O bond stretching vibrations ν_1 to ν_6 .

Isomer		E_{tot}	E_{tot}^b	ν_1^c	ν_2	ν_3	ν_4	ν_5	ν_6
C_3	<i>syn, syn, syn</i>	12.12	14.41	1591 (1)	1585 (13)	1585 (10)	1568 (1697)	1568 (1669)	1567 (1724)
C_2	<i>anti, syn, syn</i>	8.56	9.74	1591 (54)	1579 (13)	1577 (629)	1575 (808)	1571 (444)	1570 (3068)
C_s	<i>anti, anti, syn</i>	5.01	7.20	1591 (155)	1585 (727)	1579 (63)	1570 (274)	1569 (3776)	1566 (29)
C_{2h}	<i>anti, anti, anti</i>	2.65	6.79	1583 (0)	1583 (1590)	1578 (0)	1576 (17)	1564 (3360)	1560 (0)
S_6^d	<i>anti, anti, anti</i>	0.00	0.00	1581 (703)	1577 (0)	1577 (0)	1576 (0)	1575 (2106)	1575 (2117)
D_{3d}	<i>anti, anti, anti</i>	10.02	12.35 ^e	1589 (0)	1578 (86)	1578 (92)	1567 (4909)	1566 (0)	1566 (0)

^a at the B3LYP/6-311+g(d,p) level, ^b a polarisable continuum model was applied with MeCN as the solvent, ^c frequency / (cm⁻¹), intensity / (km mol⁻¹) in parentheses, ^d C_3 and C_i symmetric start geometries revert to S_6 symmetry, ^e imaginary frequency at -24 cm⁻¹.

Clearly, any *syn*-configuration increases internal energy and is therefore thermodynamically disfavoured. Even though the PCM model appears to increase the energetic preference for the S_6 conformer, all energies are within a narrow band that stretches over less than 15 kJ mol⁻¹.

¹⁴N NMR spectra of the hexanitrate complexes were recorded in dichloromethane-*d*₂. All spectra show at least three resonance lines attributable to NO₃ groups at δ (¹⁴N) / ppm \approx -7 ($\Delta\nu_{1/2}$ = 87 Hz), -44 ($\Delta\nu_{1/2}$ = 85 Hz) (**1c**), -13 ($\Delta\nu_{1/2}$ = 22 Hz), -34 ($\Delta\nu_{1/2}$ = 65 Hz), -40 ($\Delta\nu_{1/2}$ = 50 Hz) (**2c**) and -13 ($\Delta\nu_{1/2}$ = 88 Hz), -29 ($\Delta\nu_{1/2}$ = 82 Hz) (**3c**, also MeCN at -136.0, $\Delta\nu_{1/2}$ = 90 Hz). These signals are thought to arise from E(NO₃)₆²⁻ as well as the solvent-induced dissociation into E(NO₃)_{6-x}^{(2-x)-} and NO₃⁻ anions. This interpretation is supported by the predicted ¹⁴N shielding parameters obtained from the DFT (*vide supra*) calculations using the optimised structures of candidate species within the PCM model in CH₂Cl₂. For the silicon species the calculated chemical shifts relative to MeNO₂ are δ (¹⁴N) / ppm = -7 ppm (NO₃⁻) and -43 (Si(NO₃)₆²⁻), -52 (Si(NO₃)₄(NCMe)₂), -78 (Si(NO₃)₄) and -157 (MeCN) which allows the assignment of the peaks found in the solution of **1c** to NO₃⁻ and Si(NO₃)₆²⁻, respectively.

Conclusion

A synthetic route has been demonstrated leading to the previously unreported oxygen-rich, hypercoordinate, homoleptic nitrate complexes of silicon and germanium. The direct approach using (PPN)NO₃ and the tetrachloride fails to accomplish complete ligand exchange. Instead, a two-step process *via* the thermolabile tetranitrates gave the salt-like compounds containing the sought-after hexanitrate complexes. This approach avoids the use of dry, NO₂-free N₂O₅ required previously in the synthesis of polynitrates. As the size of the central *p*-block atom increases (Si < Ge < Sn), the complexes adopt an increasingly distorted octahedral geometry and the nitrate ligands adopt a $\kappa^1O / \kappa^2O,O'$ hybrid coordination mode akin to transition metal nitrate complexes. DFT calculations reveal the likely existence of rotamers due to the *syn* or *anti* arrangement of pairs of *trans*-nitrate ligands of which two types are observed in the solid state. The complex rotamer in which all nitrate ligands adopt *trans* configuration has the lowest energy at 0 K. The hypercoordinate E(NO₃)₆²⁻ complexes show greater thermal stability than either the related tetracoordinate E(NO₃)₄ nitrates or hexacoordinate chloro(nitrate) complexes. The stability gap between tetranitrate and hexanitrate species has been rationalised by comparison of structural parameters obtained from DFT. The thermal decomposition of the new hexanitrate complexes has been

interpreted in terms of NO₂ / O₂ loss accompanied with the deposition of the corresponding oxide (Si, Sn) or metal (Ge) based on the observed mass losses under controlled heating. The proof that homoleptic polynitrates of the lighter group 14 elements Si and Ge can be stabilised under ambient conditions and the noted possibility of their controlled thermally induced decomposition at elevated temperatures opens up an opportunity to study decomposition mechanisms of such energetic species and use the same synthetic method to a more diverse range of polynitrato species.

Experimental

Standard Schlenk tube, vacuum line and glove box techniques were employed throughout. NMR spectra were recorded on a Bruker Avance 250 MHz (¹H, ¹³C{¹H}, ³¹P{¹H}) or 400 MHz (solution ¹⁴N, ²⁹Si{¹H} MAS at 10 kHz) spectrometers run by TopSpin software. TGA, DSC measurements and elemental analyses were obtained at the Centre for Chemical Instrumentation and Analytical Services at Sheffield, using a Perkin Elmer 2400 CHNS/O series II elemental analyser, a Perkin-Elmer thermographic analyser (20 ml min⁻¹ N₂ protective gas) and Pyris 1 differential scanning calorimeter (both run at heating rate 10 K min⁻¹). DSC samples were prepared under argon and loaded into sealed, stainless steel, high pressure capsules (*V*_{int} = 30 μL) with Au-plated copper seals, which can operate up to 400°C and 150 bar. Onset temperatures and mass losses were calculated using the data analysis tools within instrument software. FTIR spectra were recorded between NaCl windows in the range 500-4000 cm⁻¹ using a Bruker Tensor 27 FTIR spectrometer running OPUS software, at a resolution of 2 cm⁻¹. The spectra obtained from nujol suspensions contained a number of very weak bands, which are not reported. Single crystal X-ray diffraction measurements for the structures of **3a**·2MeCN, **1c**, **2c**, **3c** and (PPN)NO₃·MeCN were recorded on a Bruker Kappa diffractometer equipped with CCD area detector and Oxford Cryosystems NHelix cryostat. Data were collected and integrated using APEX2 and Bruker SAINT, respectively. Absorption correction was applied using SADABS (APEX2). All structures were solved by direct methods (SHELXS-97) and refined using SHELXL-2014 within the Shelx software suite. H atoms were included on idealised positions (riding model) with the thermal parameters *H*_{iso} = 1.2*U*_{eq}(pivot atom). The synthesis of **1b** was adapted from a previous report.²⁶ SiCl₄, GeCl₄ and SnCl₄ (all obtained from Aldrich) were stirred over dry Na₂CO₃ and purified by trap-to-trap condensation. AgNO₃ (Engelhard) was used without further purification. (PPN)NO₃ was prepared from (PPN)Cl according to a published procedure^{49,50} and confirmed to be of high purity (elem. anal. calcd. for C₃₆H₃₀N₂O₃P₂, 600.57 g mol⁻¹, C,

72.00; H, 5.04; N, 4.66, found C, 71.92; H, 4.87; N, 4.51%). The pre-dried solvents (Grubbs)⁵¹ MeCN, Et₂O and CD₂Cl₂ were stored over CaH₂ and purified by trap-to-trap condensation prior to use. Filtration was carried out using stainless steel cannulas fitted with 24 mm glass microfiber filters (VWR).

Caution! *Although no violent reactions were encountered by us, appropriate safety measures need to be taken in attempts to prepare oxygen-rich covalent polynitrates. Filter residues other than those of the PPN salts should not be allowed to dry in the air or in vacuo and should be discarded into dilute, aqueous sodium hydroxide.*

In situ generation of Si(NO₃)₄ (1b), modified from reference 24. A Schlenk tube containing a mixture of SiCl₄ (0.250 g, 1.47 mmol) in diethyl ether (5 ml) was immersed in a cold bath at -40°C. After the ethereal solution had attained the bath temperature, a cold solution (-40°C) of AgNO₃ (1.03 g, 6.06 mmol) in acetonitrile was added rapidly, upon which AgCl is produced as a white, suspended solid. Immediately after the addition was completed, the Schlenk tube was immersed in liquid nitrogen and then allowed to warm again up to -40°C. The resultant suspension was then rapidly filtered and the filtrate collected by a second Schlenk tube containing diethyl ether (5 ml) precooled to -40°C which resulted in further precipitation of white solid. This step was repeated until no further precipitation occurred. The finally resulting colourless solution was cooled further down to -60°C and the diethyl ether removed at this temperature under a dynamic vacuum which affords an acetonitrile solution of Si(NO₃)₄ (**1b**). Solutions of **1b** were used immediately for the synthesis of **1c**. IR (MeCN, Et₂O (1:1), cm⁻¹) $\nu = 1667\text{sh (HNO}_3\text{)}, 1662\text{m}, 1617\text{m}, 1493\text{w}, 1353\text{s}, 1297\text{s}, 1153\text{s}, 1133\text{s}, 1115\text{s}.$

Synthesis of Ge(NO₃)₄ (2b). GeCl₄ (0.35 ml, 3.1 mmol) was dissolved in acetonitrile (3 ml) in a Schlenk tube and treated with a solution of AgNO₃ (2.12 g, 12.5 mmol) in acetonitrile at room temperature resulting in an immediate white precipitate, AgCl. The solution was allowed to stir for 2 h at ambient temperature and then filtered. The colourless, filtrate was collected and the majority of the solvent removed under dynamic vacuum. The evaporation residue consisted of a colourless, gel-like solid containing germanium tetranitrate (**2b**). IR (nujol, cm⁻¹) $\nu = 3224\text{w}, 3189\text{w}, 3165\text{w}, 3006\text{m}, 2300\text{s}, 2272\text{s}, 2253\text{m}, 1574\text{s}, 1550\text{s}, 1445\text{s}, 1428\text{m}, 1414\text{m}, 1367\text{m}, 1323\text{s}, 1307\text{s}, 1283\text{s}, 1032\text{m}, 948\text{s}, 819\text{w}, 786\text{m}, 763\text{m}, 709\text{w}, 692\text{m};$ (MeCN, cm⁻¹) $\nu = 1667 \text{ (HNO}_3\text{)} 1618 \text{ m}, 1558 \text{ m}, 1286 \text{ s}.$

Synthesis of Sn(NO₃)₄ (3b). The procedure for **2b** was also applied to the preparation of **3b** from SnCl₄. IR (Nujol, cm⁻¹) $\nu = 2920s, 2852s, 2294m, 2253s, 1645s, 1433vs, 1377vs, 1038s, 952m, 919s, 842m, 725m, 689w$; (MeCN, cm⁻¹) $\nu = 1667$ (HNO₃), 1592w, 1554s, 1285s.

Preparation of (PPN)₂Si(NO₃)₆ (1c). The solution of **1b**, containing approximately 1.5 mmol of **1b**, was allowed to warm to -40°C and transferred via cannula to a colourless solution of (PPN)NO₃ (1.77 g, 2.95 mmol) in acetonitrile at the same temperature resulting in a clear, pale green reaction solution and stirred for 1 h. This solution was placed under a dynamic vacuum until all acetonitrile had been evaporated leaving an off-white solid. The solid was washed with cold acetonitrile at -40°C and then dissolved by adding approximately 5 ml acetonitrile and raising the temperature to ambient temperature. Colourless, block-shaped crystals of **1c** were obtained upon reducing the temperature to -28°C within 24 h. The crystals were isolated by filtration, washing (cold acetonitrile) and drying under high vacuum, 0.568 g, 0.384 mmol, 24% with respect to SiCl₄. Solid **1c** is moderately air sensitive and decomposes in air at r.t. within *ca.* 0.5 h. Elem. anal. calcd. for C₇₂H₆₀N₈O₁₈P₄Si (1477.29 g mol⁻¹): C, 58.54; H, 4.09; N, 7.59%; found: C, 58.37; H, 3.84; N, 7.70%. DSC, $T_{on}^{ex1} = 146^{\circ}C$, $T_p^{ex1} = 154^{\circ}C$, $\Delta H^1 = -93 \text{ J g}^{-1}$, $T_{on}^{ex2} = 276^{\circ}C$, $T_p^{ex2} = 301^{\circ}C$, $\Delta H^2 = -791 \text{ J g}^{-1}$. IR (Nujol cm⁻¹) $\nu = 3164w, 1623m, 1589m, 1569vs, 1484s, 1344s, 1322vs, 1293vs, 1287vs, 1274vs, 1267vs, 1185w, 1154w, 1117vs, 1072w, 1036w, 998m, 977vs, 950s, 930vs, 824m, 798w, 752s, 724vs, 695vs, 547vs$. ¹H-NMR (CD₂Cl₂, 250 MHz) δ [ppm] = 7.65 (m, 4H), 7.45 (m, 26H). ¹⁴N{¹H} NMR (CD₂Cl₂, 29 MHz) δ [ppm] = -7.3 (rel. int. 1, $\Delta\nu_{1/2} = 87$ Hz), -43.8 (rel. int. 1.5, $\Delta\nu_{1/2} = 85$ Hz). ²⁹Si{¹H} NMR (MAS, 10 kHz) δ [ppm] = 198.4, 198.9.

Synthesis of (PPN)₂Ge(NO₃)₆ (2c). The gel (**2b**) was re-dissolved in acetonitrile and added to a solution of (PPN)NO₃ (3.19 g, 5.31 mmol) in acetonitrile. The resulting reaction solution was allowed to stir for 1 h, after which the solvent was evaporated to dryness in *vacuo* resulting in an off-white solid. The solid was washed with cold acetonitrile and then dissolved in warm (55°C) acetonitrile. Precipitation of the salt **2c** was induced by slow reduction of the solution temperature to -28°C within 24 h. Colourless, block-shaped crystals were obtained by filtration, washing and drying in *vacuo*, 1.849 g, 1.22 mmol, 40% with respect to GeCl₄, elem. anal. calcd. for C₇₂H₆₀GeN₈O₁₈P₄ (1521.79 g mol⁻¹): C, 56.83; H, 3.97; N, 7.36%; found: C, 56.43; H, 3.91; N, 6.90%. IR (Nujol, cm⁻¹) $\nu = 3055m, 1561vs, 1464m, 1298 \text{ vs}, 1291vs, 1278s, 1272vs, 1183m, 1116vs, 998m, 959vs, 953vs, 725vs, 691vs,$

532vs. $T_{\text{on}}^{\text{ex1}} = 168^{\circ}\text{C}$, $T_{\text{p}}^{\text{ex1}} = 172^{\circ}\text{C}$, $\Delta H^1 = -61 \text{ J g}^{-1}$, $T_{\text{on}}^{\text{ex2}} = 294^{\circ}\text{C}$, $T_{\text{p}}^{\text{ex2}} = 301^{\circ}\text{C}$, $\Delta H^2 = -685 \text{ J g}^{-1}$. ^1H NMR (CD_2Cl_2 , 250 MHz) δ [ppm] = 7.65 (m, 4H), 7.45 (m, 26H). $^{14}\text{N}\{^1\text{H}\}$ NMR (CD_2Cl_2 , 29 MHz) δ [ppm] = -12.7 (rel. int. 1.0, $\Delta v_{1/2} = 22 \text{ Hz}$), -34.0 (rel. int. 1.0, $\Delta v_{1/2} = 65 \text{ Hz}$), -39.7 (rel. int. 2.0, $\Delta v_{1/2} = 50 \text{ Hz}$).

Synthesis of $(\text{PPN})_2\text{Sn}(\text{NO}_3)_6 \cdot 2\text{MeCN}$ (3c**·**2MeCN**).** The same procedure was applied to the preparation of **2c** and **3c**·**2MeCN**. Colourless, block-shaped crystals (1.174 g, 0.712 mmol, 64% with respect to SnCl_4 . Elem. anal. calcd. for $\text{C}_{76}\text{H}_{66}\text{N}_{10}\text{O}_{18}\text{P}_4\text{Sn}$ ($1650.02 \text{ g mol}^{-1}$): C, 55.32; H, 4.03; N, 8.49%; found: C, 55.09; H, 3.81; N, 8.06%; m.p. $204\text{-}206^{\circ}\text{C}$. DSC, $T_{\text{on}}^{\text{endo}} = 94^{\circ}\text{C}$, $T_{\text{p}}^{\text{endo}} = 103^{\circ}\text{C}$, $\Delta H^{\text{endo}} = 12.4 \text{ J g}^{-1}$, $T_{\text{on}}^{\text{ex1}} = 182^{\circ}\text{C}$, $T_{\text{p}}^{\text{ex1}} = 221^{\circ}\text{C}$, $\Delta H^{\text{ex1}} = -583 \text{ J g}^{-1}$; $T_{\text{on}}^{\text{ex2}} = 276^{\circ}\text{C}$, $T_{\text{p}}^{\text{ex2}} = 281^{\circ}\text{C}$, $\Delta H^{\text{ex2}} = -367 \text{ J g}^{-1}$. IR (Nujol, cm^{-1}) $\nu = 3063\text{m}$, 2249w , 1589m , 1547vs , 1544vs , 1541vs , 1538vs , 1462s , 1297vs , 1290vs , 1280vs , 1272vs , 1182m , 1115s , 1026m , 969vs , 964vs , 745s , 723vs , 690vs . ^1H NMR (CD_2Cl_2 , 250MHz): δ [ppm] = 7.65 (m, 4H), 7.45 (m, 26H), 2.10 (s, 6H, CH_3CN); ^{14}N NMR (CD_2Cl_2 , 29 MHz) δ [ppm] = -12.6 (rel. int. 0.35, $\Delta v_{1/2} = 88 \text{ Hz}$), -29.3 (rel. int. 1.0, $\Delta v_{1/2} = 82 \text{ Hz}$), -136.0 (rel. int. 1.0, CH_3CN , $\Delta v_{1/2} = 90 \text{ Hz}$).

Acknowledgements

Prof. B. T. Pickup, University of Sheffield, is thanked for help with DFT calculations, the University of Sheffield (postgraduate studentship to BP) and the EPSRC (postdoctoral fellowship to MD, EP/E054978/1) are thanked for their support.

Supporting information containing crystallographic and computational details, IR and NMR spectra and TA traces is available free of charge from the ACS website at DOI: Crystallographic data for this paper (CCDC 1479375, **1c**; 1479376, **3c**·**2MeCN**; 1479377, **2c**; 1479378, **3a**; 1481642, $(\text{PPN})\text{NO}_3 \cdot \text{MeCN}$) can be obtained free of charge from The Cambridge Crystallographic Data Centre via www.ccdc.cam.ac.uk/structures.

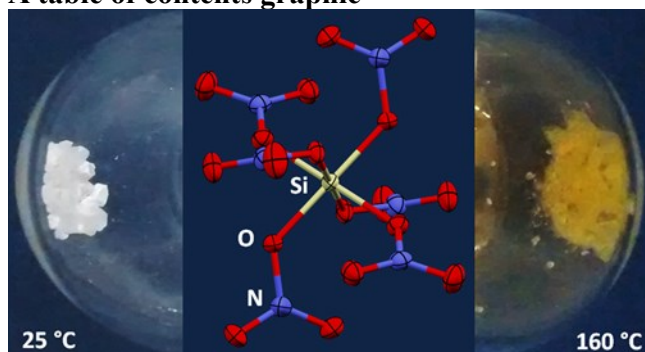
References

- (1) Garner, C. D.; Sutton, D.; Wallwork, S. C. *J. Chem. Soc. A* **1967**, 1949-1954.
- (2) Addison, C. C. *Coord. Chem. Rev.* **1966**, *1*, 58-65.
- (3) Wickleder, M. S.; Gerlach, F.; Gagelmann, S.; Bruns, J.; Fenske, M.; Al-Shamery, K. *Angew. Chem. Int. Ed.* **2012**, *51*, 2199-2203.
- (4) Colombo, D. G.; Gilmer, D. C.; Young, V. G., Jr.; Campbell, S. A.; Gladfelter, W. L. *Chem. Vap. Deposition* **1998**, *4*, 220-222.
- (5) Addison, C. C.; Logan, N. *Adv. Inorg. Chem. Radiochem.* (H. J. Emeleus and A. G. Sharpe, editors) **1964**, *6*, 71-142.
- (6) Addison, C. C.; Simpson, W. B. *J. Chem. Soc.* **1965**, 598-602.

- (7) Guibert, C. R.; Marshall, M. D. *J. Am. Chem. Soc.* **1966**, *88*, 189-190.
- (8) Shirokova, G. N.; Rosolovskii, V. Ya. *Russ. J. Inorg. Chem.* **1971**, *16*, 767-768.
- (9) Addison, C.; Boorman, P.; Logan, N. *J. Chem. Soc. A* **1966**, 1434-1437.
- (10) Krivtsov, N. V.; Shirokova, G. N.; Zhuk, S. Ya.; Rosolovskii, V. Ya. *Russ. J. Inorg. Chem.* **1971**, *16*, 1402-1403.
- (11) Shirokova, G. N., Rosolovskii, V. Ya. *Russ. J. Inorg. Chem.* **1971**, *16*, 1699.
- (12) Jones, C. B.; Haiges, R.; Schroer, T.; Christe, K. O. *Angew. Chem. Int. Ed.* **2006**, *45*, 4981-4984.
- (13) K. O. Christe *Propellants, Explos., Pyrotech.* **2007**, *32*, 194-204.
- (14) Colombo, D. G.; Young, V. G. Jr.; Gladfelter, W. L. *Inorg. Chem.* **2000**, *39*, 4621-4624.
- (15) Ivanov-Emin, B. N.; Odinets, Z. K.; Yushchenko, S. F.; Zaitsev, B. E.; Ezhov, A. I. *Russ. J. Inorg. Chem.* **1975**, *20*, 843-846.
- (16) Krivtsov, N. V.; Shirokova, G. N.; Zhuk, S. Ya.; Rosolovskii, V. Ya. *Russ. J. Inorg. Chem.* **1976**, *21*, 1409-1410.
- (17) Shirokova, G. N.; Rosolovskii, V. Ya. *Russ. J. Inorg. Chem.* **1971**, *16*, 808-811.
- (18) Shirokova, G. N.; Rosolovskii, V. Ya. *Russ. J. Inorg. Chem.* **1971**, *16*, 1106-1109.
- (19) Shirokova, G. N.; Zhuk, S. Ya.; Rosolovskii, V. Ya. *Russ. J. Inorg. Chem.* **1975**, *20*, 856-859.
- (20) D'yachenko, O. A.; Atovmyan, L. O. *J. Struct. Chem.* **1975**, *16*, 73-78.
- (21) Potts, D.; Sharma, H. D.; Carty, A. J.; Walker, A. *Inorg. Chem.* **1974**, *13*, 1205-1211.
- (22) Shirokova, G. N.; Zhuk, S. Ya.; Rosolovskii, V. Ya. *Russ. J. Inorg. Chem.* **1976**, *21*, 1459-1461.
- (23) Shirokova, G. N.; Zhuk, S. Ya.; Rosolovskii, V. Ya. *Russ. J. Inorg. Chem.* **1976**, *21*, 527-529.
- (24) Tranter, G. C.; Addison, C. C.; Sowerby, D. B. *J. Inorg. Nucl. Chem.* **1968**, *30*, 97-103.
- (25) Bagnall, K. W.; Brown, D.; Du Preez, J. G. H. *J. Chem. Soc.* **1964**, 5523-5525.
- (26) Beattie, I. R.; Leigh, G. J. *J. Chem. Soc.* **1961**, 4249-4250.
- (27) Schmeisser, M. *Angew. Chem.* **1955**, *67*, 493-501.
- (28) Addison, C. C.; Simpson, W. B. *J. Chem. Soc.* **1965**, 598-602.
- (29) Eaborn, C.; Hitchcock, P. B.; Lickiss, P. D.; Pidcock, A.; Safa, K. D. *J. Chem. Soc., Dalton Trans.* **1984**, 2015-2017.
- (30) Metz, S.; Burschka, C.; Tacke, R. *Organometallics* **2008**, 6032-6034.
- (31) Drake, J. E.; Henderson, H. E. *J. Inorg. Nucl. Chem.* **1978**, *40*, 137-139.
- (32) Campbell, R.; Davis, M. F.; Fazakerley, M.; Portius, P. *Chem. Eur. J.* **2015**, *51*, 18690-18698.
- (33) Filippou, A. C.; Portius, P.; Neumann, D. U.; Wehrstedt, K.-D. *Angew. Chem. Int. Ed.* **2000**, *39*, 4333-4336.
- (34) Filippou, A. C.; Portius, P.; Schnakenburg, G. *J. Am. Chem. Soc.* **2002**, *124*, 12396-12397.
- (35) Haiges, R.; Buszek, R. J.; Boatz, J. A.; Christe, K. O. *Angew. Chem. Int. Ed.*, **2014**, *53*, 8200-8205.
- (36) Portius, P.; Fowler, P. W.; Adams, H.; Todorova, T. Z. *Inorg. Chem.* **2008**, *47*, 12004-12009.
- (37) Haiges, R.; Boatz, J. A.; Christe, K. O. *Angew. Chem. Int. Ed.*, **2010**, *49*, 8008-8012.
- (38) Klapötke, T. M.; Krumm, B.; Scherr, M.; Haiges, R.; Christe, K. O. *Angew. Chem. Int. Ed.*, **2007**, *46*, 8686-8690.
- (39) Haiges, R.; Boatz, J. A.; Schroer, T.; Yousufuddin, M.; Christe, K. O. *Angew. Chem. Int. Ed.*, **2006**, *45*, 4830-4835.
- (40) Haiges, R.; Boatz, J. A.; Bau, R.; Schneider, S.; Schroer, T.; Yousufuddin, M.; Christe, K. O. *Angew. Chem. Int. Ed.*, **2005**, *44*, 1860-1865.
- (41) Haiges, R.; Boatz, J. A.; Vij, A.; Vij, V.; Gerken, M.; Schneider, S.; Schroer, T.; Yousufuddin, M.; Christe, K. O. *Angew. Chem. Int. Ed.*, **2004**, *43*, 6676-6680.
- (42) Haiges, R.; Boatz, J. A.; Schneider, S.; Schroer, T.; Yousufuddin, M.; Christe, K. O. *Angew. Chem. Int. Ed.*, **2004**, *43*, 3148-3152.
- (43) Klapötke, T. M.; Krumm, B.; Mayer, P.; Schwab, I. *Angew. Chem. Int. Ed.* **2003**, *42*, 5843-5946.
- (44) Haiges, R.; Rahm, M.; Dixon, D. A.; Garner, E. B.; Christe, K. O. *Inorg. Chem.* **2012**, *51*, 1127-1141.
- (45) Haiges, R.; Boatz, J. A.; Williams, J. M.; Christe, K. O. *Angew. Chem. Int. Ed.* **2011**, *50*, 8828-8833.

- (46) Haiges, R.; Boatz, J. A.; Yousufuddin, M.; Christe, K. O. *Angew. Chem. Int. Ed.* **2007**, *46*, 2869-2874.
- (47) Mantina, M.; Chamberlin, A. C.; Valero, R.; Cramer, C. J.; Truhlar, D. G. *J. Phys. Chem. A* **2009**, *113*, 5806-5812.
- (48) Bondi, A. *J. Phys. Chem.* **1964**, *68*, 441-451.
- (49) Kukushkin, V. Y.; Moiseev, A. I. *Inorg. Chim. Acta* **1990**, *176*, 79-81.
- (50) Martinsen, A.; Songstad, J. *Acta Chem. Scand. A* **1977**, *31*, 645-650.
- (51) Pangborn, A. B.; Giardello, M. A.; Grubbs, R. H.; Rosen, R. K.; Timmers, F. J. *Organometallics* **1996**, *15*, 1518-1520.

A table of contents graphic



Synopsis

The novel homoleptic nitrate complexes $\text{Si}(\text{NO}_3)_6^{2-}$, $\text{Ge}(\text{NO}_3)_6^{2-}$ and $\text{Ge}(\text{NO}_3)_4$ were synthesised and characterised and the structures of the hexanitratates including that of $\text{Sn}(\text{NO}_3)_6^{2-}$ determined crystallographically. The new $\text{E}(\text{NO}_3)_6^{2-}$ complexes are surprisingly thermally stable and unreactive in contrast to the related tetranitratates. DFT calculations were employed to investigate their distorted octahedral coordination geometry